Journal of Solid State Chemistry 184 (2011) 2466–2471

Contents lists available at ScienceDirect

Journal of Solid State Chemistry

journal homepage: www.elsevier.com/locate/jssc

Synthesis, crystal structures and photoluminescence properties of new oxyborates, $Mg_5NbO_3(BO_3)_3$ and $Mg_5TaO_3(BO_3)_3$, with novel warwickite-type superstructures

Tetsuya Kawano, Hisanori Yamane *

Institute of Multidisciplinary Research for Advanced Materials, Tohoku University, 2-1-1 Katahira, Aoba-ku, Sendai 980-8577, Japan

ARTICLE INFO

Article history:
Received 16 April 2011
Received in revised form
12 July 2011
Accepted 13 July 2011
Available online 23 July 2011

Keywords:
Synthesis
Magnesium niobium (V) oxyborate
Magnesium tantalum (V) oxyborate
X-ray diffraction
Crystal structure analysis
Photoluminescence

ABSTRACT

Single crystals of new oxyborates, $Mg_5NbO_3(BO_3)_3$ and $Mg_5TaO_3(BO_3)_3$, were prepared at 1370 °C in air using B_2O_3 as a flux. They were colorless and transparent with block shapes. X-ray diffraction analysis of the single crystals revealed $Mg_5NbO_3(BO_3)_3$ and $Mg_5TaO_3(BO_3)_3$ to be isostructural. The X-ray diffraction reflections were indexed to the orthorhombic *Pnma* (No. 62) system with $a=9.3682(3)$ Å, $b=9.4344(2)$ Å, $c=9.3379(3)$ Å and $Z=4$ for $Mg_5NbO_3(BO_3)_3$ and $a=9.3702(3)$ Å, $b=9.4415(3)$ Å, $c=9.3301(2)$ Å and $Z=4$ for $Mg_5TaO_3(BO_3)_3$. The crystal structures of $Mg_5NbO_3(BO_3)_3$ and $Mg_5TaO_3(BO_3)_3$ are novel warwickite-type superstructures having ordered arrangements of Mg and Nb/Ta atoms. Polycrystals of $Mg_5NbO_3(BO_3)_3$ prepared by solid state reaction at 1200 °C in air showed broad blue-to-green emission with a peak wavelength of 470 nm under 270 nm ultraviolet excitation at room temperature.

1. Introduction

Various kinds of compounds containing borate groups have been found and classified [1,2]. Many of them have been studied and used for nonlinear optical (NLO) materials and host materials of lasers and phosphors [3,4]. In the A_2O–$M^V_2O_5$–B_2O_3 (A=Alkali metals; M^V=Nb, Ta) systems, NLO properties of $AM^VOB_2O_5$ (A=K, Rb, Cs, Tl; M^V=Nb, Ta) [5], photocatalytic properties of $K_3Ta_3O_6(BO_3)_2$ [6] and ferroelectric, ferroelastic and superionic properties of $K_3Nb_3O_6(BO_3)_2$ [7] have been investigated. A number of oxyborates with the warwickite-type structure, $A_2[O(BO_3)]$, were synthesized in M^{II}–M^{III}–B–O systems. The magnetic properties of $MgCr^{3+}OBO_3$, $MgFe^{3+}OBO_3$, $Ni^{2+}ScOBO_3$, $Mn^{2+}ScOBO_3$, $Fe^{2+}Fe^{3+}OBO_3$ and $Mn^{2+}Mn^{3+}OBO_3$ [8,9] and the luminescence properties of $M^{II}LaOBO_3$: Pb^{2+} (M^{II}=Ca, Sr) and $CaYOBO_3$: Ln^{3+} (Ln=Eu, Gd, Tb, Ce) [10,11] have been reported. However, there has been no report on compounds with the warwickite-type and its related structures in Mg^{II}–M^V–B–O (M=Nb, Ta) systems.

Pentavalent niobium (Nb^{5+}) and tantalum (Ta^{5+}) ions, as well as Ti^{4+}, Zr^{4+}, V^{5+}, Mo^{6+} and W^{6+} ions with d^0 closed-shell configuration, are known to be luminescence centers for phosphors [12]. The emissions are attributed to charge transfer (CT) transitions between M^{p+}–O^{2-} ions (M: d^0 transition metal elements). Luminescence properties and crystallographic aspects of niobates and tantalates have been summarized by Wachtel [13] and Blasse et al. [14–17]. $MgNb_2O_6$, $Mg_4Nb_2O_9$ and $CaTa_2O_6$ show host luminescence at room temperature [13]. Emissions at low temperatures less than 15 K have also been observed for $Ba_3NaM^VO_6$ [17], $Ba_3SrM^V_2O_9$ [18], $NbPO_5$ [19], $MgNb_2(P_2O_7)_3$ [20], $K_2(NbO)_2Si_4O_{12}$ [21], and $Ba_5M^V_4O_{15}$ (M^V=Nb, Ta) [22]. These niobates and tantalates are excited by ultraviolet rays of ~200–300 nm and show broad emission spectra with peak wavelengths of ~350–500 nm. The zur Loye group found new niobates and tantalates, Ln_2KNbO_6 (Ln=La, Nd) [23], $Sr_3Li_6M^V_2O_{11}$ [24] and $Sr_3NaM^VO_6$ (M^V=Nb, Ta) [25], and reported their photoluminescence properties at room temperature.

In the present study, we explored new compounds in the MgO–$M^V_2O_5$–B_2O_3 (M^V=Nb, Ta) systems and synthesized two new oxyborates: $Mg_5NbO_3(BO_3)_3$ and $Mg_5TaO_3(BO_3)_3$. The present paper reports the preparation, crystal structures and photoluminescence properties of these compounds.

2. Experimental

2.1. Synthesis of samples

Starting powders of MgO (99.9%, Rare Metallic), Nb_2O_5 (99.9%, Wako Pure Chem., Ind.), Ta_2O_5 (99.9%, Wako Pure Chem., Ind.) and H_3BO_3 (99.99%, Sigma-Aldrich) were weighed with molar ratios of $Mg:M^V:B=5:1:3.3$ (M^V=Nb, Ta). An excess of 10 mol% of H_3BO_3

* Corresponding author. Fax: +81 22 217 5813.
E-mail address: yamane@tagen.tohoku.ac.jp (H. Yamane).

0022-4596/$ - see front matter © 2011 Elsevier Inc. All rights reserved.
doi:10.1016/j.jssc.2011.07.022

was added to the starting mixtures in consideration of the volatilization loss of B_2O_3 during heating. The powders were mixed in an agate mortar with a pestle, pressed into pellets and placed on a platinum (Pt) plate. The pellets were firstly heated at 1000 °C for 6 h in air. They were then crushed and pelletized and finally heated at 1200 °C for 24 h in air. As references of photoluminescence properties, polycrystalline $MgNb_2O_6$ and $Mg_4Nb_2O_9$ were also prepared from mixtures of the starting powders with stoichiometric molar ratios by solid state reaction at 1200 °C for 15–30 h in air.

Single crystals of $Mg_5M^VO_3(BO_3)_3$ (M^V=Nb, Ta) were prepared using B_2O_3 as a flux. Approximately 50 mg of the polycrystalline samples, prepared by the above-mentioned methods, and 50 mg of H_3BO_3 were weighed, mixed and put into Pt boats. The mixtures were heated at 1370 °C for 1–3 h and cooled to 1270 °C for 10 h. They were then cooled to room temperature at a rate of about 15 °C min^{-1}.

Polycrystalline sample prepared in the $MgO–Nb_2O_5–B_2O_3$ system was analyzed by inductively coupled plasma–optical emission spectrometry and the helium gas carrier fusion-infrared absorption method using an IRIS Advantage DUO (Thermo Fisher Scientific) analyzer and a TC-436 (LECO) analyzer, respectively.

2.2. Characterization

X-ray diffraction (XRD) data of $Mg_5M^VO_3(BO_3)_3$ (M^V=Nb, Ta) single crystals were collected using Mo $K\alpha$ radiation with a graphite monochromator and an imaging plate on a single-crystal X-ray diffractometer (Rigaku, R-AXIS RAPID-II). Diffraction-data collection and unit-cell refinement were performed by the PROCESS-AUTO program [26]. Absorption correction was performed by the NUMABS program [27].

The crystal structures were solved by the charge flipping method using the Superflip program [28] and refined by the full-matrix least-squares on F^2 using the SHELXL-97 program [29]. All calculations were carried out on a personal computer using the WinGX software package [30]. The atomic coordinates were standardized by the STRUCTURE TIDY program [31].

The pellets of the polycrystalline samples were powdered and characterized by powder XRD using Cu $K\alpha$ radiation with a graphite monochromator mounted on a powder diffractometer (Rigaku, RINT2000). The crystal structure parameters of $Mg_5NbO_3(BO_3)_3$ in a polycrystalline sample were refined using the RIETAN-FP program [32]. The crystal structures were illustrated by the VESTA program [33].

The photoluminescence (PL) excitation and emission spectra of $Mg_5NbO_3(BO_3)_3$ were measured at room temperature with a fluorescence spectrophotometer (Hitachi, F-4500) equipped with a 150-W xenon lamp as an excitation source. The quantum efficiencies of the solid solutions were measured at room temperature using a quantum efficiency measurement system (Otsuka Electronics, QE-1000). $BaSO_4$ was used as a reference sample.

3. Results and discussion

3.1. Crystal structures of $Mg_5M^VO_3(BO_3)_3$ (M^V=Nb, Ta)

The starting mixtures of the $MgO–M^V_2O_5–B_2O_3$ (M^V=Nb, Ta) systems were melted at 1370 °C. The melts spread on the surface of the Pt boats, and colorless and transparent single crystals with block shapes and ranging in size up to 1 mm were obtained by slow cooling.

The data collection and refinement results for the single crystals are listed in Table 1. Single-crystal XRD reflections were indexed with the orthorhombic space group *Pnma* with unit-cell parameters of a=9.3682(3) Å, b=9.4344(2) Å and c=9.3379(3) Å for M^V=Nb and a=9.3702(3) Å, b=9.4415(3) Å and c=9.3301(2) Å for M^V=Ta. The crystal structures were analyzed with the same model and the structural chemical formulae of $Mg_5NbO_3(BO_3)_3$ and $Mg_5TaO_3(BO_3)_3$.

Table 1
Crystal data and refinement results for $Mg_5MO_3(BO_3)_3$ (M=Nb, Ta).

Chemical formula	$Mg_5NbO_3(BO_3)_3$	$Mg_5TaO_3(BO_3)_3$
Formula weight, M_r (g mol^{-1})	438.89	526.93
Temperature, T (°C)	25(2)	25(2)
Crystal system	Orthorhombic	Orthorhombic
Space group	*Pnma* (No. 62)	*Pnma* (No. 62)
Unit cell dimensions (Å)	a=9.3682(3)	a=9.3702(3)
	b=9.4344(2)	b=9.4415(3)
	c=9.3379	c=9.3301(2)
Unit cell volume, V (Å^3)	825.32(4)	825.42(4)
Z	4	4
Calculated density, D_{cal} (Mg m^{-3})	3.532	4.240
Radiation wavelength, λ (Å)	0.71073 (Mo $K\alpha$)	0.71073 (Mo $K\alpha$)
Crystal form, color	Block, colorless	Block, colorless
Absorption correction	Numerical	Numerical
Absorption coefficient, μ (mm^{-1})	1.922	13.78
Crystal size (mm^3)	0.07 × 0.08 × 0.09	0.09 × 0.08 × 0.06
Limiting indices	$-11 \le h \le 12$	$-12 \le h \le 12$
	$-12 \le k \le 12$	$-11 \le k \le 12$
	$-12 \le l \le 12$	$-12 \le l \le 12$
F_{000}	848	976
θ range for data collection (°)	3.1–27.5	3.1–27.5
Reflections collected/unique	7625/1000	7642/1002
R_{int}	0.0264	0.0297
Data/restraints/parameters	1000/0/98	1002/0/98
Weight parameters, a, b	0.0205, 0.6763	0.0126, 1.1327
Goodness-of-fit on F^2, S	1.221	1.187
$R1$, $wR2$ ($I > 2\sigma(I)$)	0.0169, 0.0453	0.0132, 0.0317
$R1$, $wR2$ (all data)	0.0195, 0.0460	0.0144, 0.0321
Largest diff. peak and hole, $\Delta\rho$ (e Å^{-3})	0.583, −0.370	0.772, −0.614

$R1=\Sigma||F_o|-|F_c||/\Sigma|F_o|$. $wR2=[\Sigma w(F_o^2-F_c^2)^2/\Sigma(wF_o^2)^2]^{1/2}$, $w=1/[\sigma^2(F_o^2)+(aP)^2+bP]$, where F_o is the observed structure factor, F_c is the calculated structure factor, σ is the standard deviation of F_c^2, and $P=(F_o^2+2F_c^2)/3$. $S=[\Sigma w(F_o^2-F_c^2)^2/(n-p)]^{1/2}$, where n is the number of reflections and p is the total number of parameters refined.

The atomic coordinates, selected bond lengths and anisotropic displacement parameters of $Mg_5M^VO_3(BO_3)_3$ (M^V=Nb, Ta) are listed in Tables 2–4. Isotropic displacement parameters were refined for the B atoms. Fig. 1 shows the coordination environments for the Mg, Nb, B and O atoms in $Mg_5NbO_3(BO_3)_3$. In the asymmetric unit, there are one Nb site, three Mg sites, two B sites and eight O sites. The Nb1, Mg3, B1, O1, O2, O3 and O7 atoms are at 4c (x, 1/4, z) special positions with site symmetries of (.m.), and the other atoms are at 8d (x, y, z) general positions. The Nb atom is coordinated by seven O atoms, the Mg atoms are coordinated by six O atoms, and B atoms are coordinated by three O atoms. The bond valence sums [34,35] listed in Table 3 suggest that the valences of Nb/Ta, Mg and B are +5, +2 and +3, respectively.

Seven-coordinated Nb/Ta atoms are less common but occur in $LaNb_5O_{14}$ [36] and a superstructure phase of L-Ta_2O_5 (19L-Ta_2O_5) [37], for examples. The Nb1/Ta1–O1 distances of 1.8731(14)–2.447(2)/1.8872(17)–2.457(3) Å observed in $Mg_5M^VO_3(BO_3)_3$ (M^V=Nb, Ta) are in accordance with Nb/Ta–O distances of (Nb/Ta)O_7 in $LaNb_5O_{14}$ (1.896–2.435 Å) and L-Ta_2O_5 (1.941(5)–2.55(2) Å).

The crystal structure of $Mg_5NbO_3(BO_3)_3$ is compared with that of $Mg_3TiO_2(BO_3)_2$ (warwickite) [38] in Fig. 2. The framework structures of both $Mg_5NbO_3(BO_3)_3$ and $Mg_3TiO_2(BO_3)_2$ closely resemble each other. Four edge-sharing MO_6 octahedra form M_4O_{18} units (M=Mg, Nb, Ti), which compose layers parallel to the (0 1 0) planes. Adjacent layers are linked along the b axes by sharing common edges.

Table 2
Atomic coordinates and isotropic and equivalent isotropic displacement parameters (U_{eq}, U_{iso}) for $Mg_5MO_3(BO_3)_3$ (M=Nb, Ta).

Atom	Site	x	y	z	U^*_{eq}, U_{iso}/Å^2
M=Nb					
Nb1	4*c*	0.09793(3)	1/4	0.08630(3)	0.00438(9)*
Mg1	8*d*	0.12534(7)	0.58426(7)	0.07296(7)	0.00546(16)*
Mg2	8*d*	0.40192(7)	0.07637(7)	0.17866(7)	0.00658(16)*
Mg3	4*c*	0.10160(10)	1/4	0.69114(10)	0.0053(2)*
B1	4*c*	0.1783(3)	1/4	0.3705(3)	0.0058(6)
B2	8*d*	0.1737(3)	0.5885(2)	0.3736(2)	0.0053(4)
O1	4*c*	0.0348(2)	1/4	0.3405(2)	0.0073(4)*
O2	4*c*	0.2364(2)	1/4	0.5033(2)	0.0060(4)*
O3	4*c*	0.2606(2)	1/4	0.2443(2)	0.0062(4)*
O4	8*d*	0.02833(15)	0.58835(14)	0.36952(15)	0.0069(3)*
O5	8*d*	0.25267(15)	0.58350(13)	0.24908(15)	0.0061(3)*
O6	8*d*	0.25792(15)	0.09228(14)	0.00736(15)	0.0062(3)*
O7	4*c*	0.5208(2)	1/4	0.6034(2)	0.0055(4)*
O8	8*d*	0.49166(16)	0.08498(14)	0.38096(14)	0.0053(3)*
M=Ta					
Ta1	4*c*	0.100986(15)	1/4	0.085433(16)	0.00434(6)*
Mg1	8*d*	0.12321(10)	0.58467(9)	0.07333(10)	0.00404(19)*
Mg2	8*d*	0.40254(9)	0.07625(10)	0.18014(10)	0.00613(19)*
Mg3	4*c*	0.10166(13)	1/4	0.69081(14)	0.0063(3)*
B1	4*c*	0.1782(5)	1/4	0.3705(5)	0.0062(8)
B2	8*d*	0.1728(3)	0.5886(3)	0.3733(3)	0.0046(6)
O1	4*c*	0.0361(3)	1/4	0.3406(3)	0.0083(6)*
O2	4*c*	0.2372(3)	1/4	0.5039(3)	0.0056(5)*
O3	4*c*	0.2608(3)	1/4	0.2449(3)	0.0059(5)*
O4	8*d*	0.0287(2)	0.58812(19)	0.3706(2)	0.0070(4)*
O5	8*d*	0.25231(19)	0.58285(17)	0.2492(2)	0.0061(4)*
O6	8*d*	0.25789(18)	0.09440(19)	0.0074(2)	0.0056(4)*
O7	4*c*	0.5214(3)	1/4	0.6050(3)	0.0051(5)*
O8	8*d*	0.49193(19)	0.08524(18)	0.38112(19)	0.0044(4)*

*$U_{eq}=(\sum_i \sum_j U_{ij}\, a_i^* a_j^*\, \boldsymbol{a}_i \cdot \boldsymbol{a}_j)/3$.

Table 3
Selected bond lengths (l_{M-O}/Å) and bond valence sums (V_i), for $Mg_5MO_3(BO_3)_3$ (M=Nb, Ta).

	M=Nb	M=Ta		M=Nb	M=Ta
M1–O8^{i}	1.8731(14)	1.8872(17)	Mg1–O5	2.0317(15)	2.038(2)
M1–O8^{ii}	1.8731(14)	1.8872(17)	Mg1–O8^{i}	2.0743(15)	2.066(2)
M1–O7^{ii}	1.913(2)	1.927(3)	Mg1–O7^{iv}	2.0978(15)	2.0880(19)
M1–O3	2.1212(19)	2.111(3)	Mg1–O8^{v}	2.1014(15)	2.093(2)
M1–O6^{iii}	2.2369(14)	2.2022(17)	Mg1–O2^{iv}	2.1322(15)	2.1372(19)
M1–O6	2.2369(14)	2.2022(17)	Mg1–O6^{iii}	2.1661(15)	2.197(2)
M1–O1	2.447(2)	2.457(3)	V_{Mg1}	2.01	2.00
V_{M1}	4.84	4.96			
Mg2–O4^{vi}	2.0050(15)	2.008(2)	Mg3–O4^{viii}	2.0318(15)	2.039(2)
Mg2–O1^{vii}	2.0654(14)	2.0724(18)	Mg3–O4^{ix}	2.0318(15)	2.039(2)
Mg2–O8	2.0692(15)	2.055(2)	Mg3–O7^{x}	2.063(2)	2.048(3)
Mg2–O6	2.0979(15)	2.113(2)	Mg3–O5^{xi}	2.1504(15)	2.1585(19)
Mg2–O5^{iii}	2.1592(15)	2.1570(19)	Mg3–O5^{xii}	2.1504(15)	2.1585(19)
Mg2–O3	2.1935(14)	2.1955(19)	Mg3–O2	2.162(2)	2.158(3)
V_{Mg2}	2.04	2.03	V_{Mg3}	2.03	2.02
B1–O2	1.354(4)	1.362(5)	B2–O4	1.363(3)	1.351(4)
B1–O1	1.373(4)	1.360(5)	B2–O5	1.379(3)	1.378(4)
B1–O3	1.409(4)	1.404(5)	B2–O6^{xiii}	1.404(2)	1.411(3)
V_{B1}	2.95	2.97	V_{B2}	2.92	2.94

Symmetry codes: (i) $x-1/2$, $-y+1/2$, $-z+1/2$; (ii) $x-1/2$, y, $-z+1/2$; (iii) x, $-y+1/2$, z; (iv) $-x+1/2$, $-y+1$, $z-1/2$; (v) $-x+1/2$, $y+1/2$, $z-1/2$; (vi) $x+1/2$, $-y+1/2$, $-z+1/2$; (vii) $x+1/2$, y, $-z+1/2$; (viii) $-x$, $y-1/2$, $-z+1$; (ix) $-x$, $-y+1$, $-z+1$; (x) $x-1/2$, y, $-z+3/2$; (xi) $-x+1/2$, $-y+1$, $z+1/2$; (xii) $-x+1/2$, $y-1/2$, $z+1/2$; (xiii) $-x+1/2$, $y+1/2$, $z+1/2$.
Bond valence parameters: Mg^{2+}: 1.693 Å, Nb^{5+}: 1.911 Å, Ta^{5+}: 1.920 Å, B^{3+}: 1.371 Å.

The atomic arrangements in the layers of M_4O_{18} units (M=Mg, Nb, Ti) are shown in Fig. 3. Ti atoms of $Mg_3TiO_2(BO_3)_2$ statistically occupy the Ti/Mg mixed site with the occupancies of Ti/Mg=0.5/0.5 (Fig. 3(b)) [38]. An ordered arrangement of Mg and Nb atoms at the middle two columns of the layers in $Mg_5NbO_3(BO_3)_3$ forms a novel warwickite-type superstructure. The *b*-axis length of $Mg_5NbO_3(BO_3)_3$, 9.4344(2) Å, is about three times as long as that of $Mg_3TiO_2(BO_3)_2$, 3.10080(14) Å. $Mg_5NbO_3(BO_3)_3$ and $Mg_5TaO_3(BO_3)_3$ are the first compounds of Nb(V) and Ta(V) with novel warwickite-type superstructures.

3.2. Preparation of polycrystalline samples

The preparations of $Mg_5M^VO_3(BO_3)_3$ (M^V=Nb, Ta) polycrystalline samples were attempted for characterization of their luminescence properties. Fig. 4 shows observed and calculated powder XRD patterns of the sample with M^V=Nb. The Rietveld analysis revealed that the sample consisted of $Mg_5NbO_3(BO_3)_3$ and less than 1 mass% of $Mg_4Nb_2O_9$. The refinement results and the atomic coordinates of $Mg_5NbO_3(BO_3)_3$ by the Rietveld analysis are listed in the supplement Tables (Tables S1 and S2, respectively). The refined unit cell parameters, atomic coordinates and estimated bond valence sums were consistent with those refined using single-crystal data (Tables 1–3).

The results of the chemical analysis for the polycrystalline sample with M^V=Nb were Mg: 27.5(1) %, Nb: 21.0(1) %, B: 7.35(1) %, O: 43.5(1) % and total: 99.3(2) % in weight. The composition agreed well with the ideal composition of $Mg_5NbO_3(BO_3)_3$, Mg: 27.7%, Nb: 21.2%, B: 7.39%, O: 43.7%.

The polycrystalline $Mg_5TaO_3(BO_3)_3$ single phase was not obtained with the starting materials of binary oxides and H_3BO_3 in the present study. We also attempted to prepare the single phase using magnesium borates and magnesium tantalates as starting materials in order to prevent the evaporation of B_2O_3 during heating. The synthesis of $Mg_5TaO_3(BO_3)_3$ could be expected by the following chemical reactions:

$$3Mg_2B_2O_5 + Mg_4Ta_2O_9 \rightarrow 2Mg_5TaO_3(BO_3)_3,$$

$$3Mg_3B_2O_6 + MgTa_2O_6 \rightarrow 2Mg_5TaO_3(BO_3)_3.$$

These starting compounds were prepared by solid state reaction at 1000–1200 °C for 15–30 h in air. They were weighed with the stoichiometric ratios and heated at 1200–1300 °C for 12–60 h in air. The XRD reflections of the sample prepared from $Mg_3B_2O_6$ and $MgTa_2O_6$ at 1300 °C were indexed with the cell parameters of $Mg_5TaO_3(BO_3)_3$, $Mg_4Ta_2O_9$ and MgO. $Mg_4Ta_2O_9$ would be thermodynamically more stable than $Mg_5TaO_3(BO_3)_3$, and $Mg_2B_2O_5$ would decompose into MgO and B_2O_3. The B_2O_3 evaporated from the samples during heating.

3.3. Photoluminescence of polycrystalline samples

The PL spectra of the sample containing $Mg_5NbO_3(BO_3)_3$ and less than 1 mass% of $Mg_4B_2O_9$ are shown in Fig. 5 with those of $MgNb_2O_6$ and $Mg_4Nb_2O_9$ prepared as references. Broad blue-to-green emission with a peak wavelength of 470 nm and a quantum efficiency η of 0.07 were observed for $Mg_5NbO_3(BO_3)_3$ under a 270 nm excitation (Fig. 5(a)). The emission spectrum was similar to that of $MgNb_2O_6$ with λ_{ex}=275 nm and λ_{em}=460 nm (Fig. 5(b)). As shown in Fig. 5(c), the peak wavelengths of the excitation and emission spectra of $Mg_4Nb_2O_9$, λ_{ex}=250 nm and λ_{em}=385 nm, were shorter than those of $Mg_5NbO_3(BO_3)_3$ and $MgNb_2O_6$. This indicated that the trace amount of $Mg_4Nb_2O_9$ included in the sample did not change the emission spectrum shown in Fig. 5(a).

The host luminescence of $MgNb_2O_6$ and $Mg_4Nb_2O_9$ has been ascribed to the CT transitions between Nb^{5+} and O^{2-} ions of NbO_6 octahedra [14]. The emission of $Mg_5NbO_3(BO_3)_3$ could also be attributed to the CT transitions in the NbO_7 polyhedra. To the best

Table 4
Anisotropic displacement parameters (U_{ij}/Å^2), $Mg_5MO_3(BO_3)_3$ (M=Nb, Ta).

Atom	Site	U_{11}	U_{22}	U_{33}	U_{12}	U_{13}	U_{23}
M=Nb							
Nb1	4*c*	0.00384(14)	0.00461(14)	0.00470(13)	0	−0.00062(10)	0
Mg1	8*d*	0.0065(3)	0.0044(3)	0.0055(3)	−0.0001(2)	−0.0020(3)	0.0004(2)
Mg2	8*d*	0.0059(3)	0.0069(3)	0.0070(3)	0.0001(3)	−0.0009(3)	−0.0003(2)
Mg3	4*c*	0.0048(5)	0.0052(4)	0.0058(4)	0	−0.0002(4)	0
O1	4*c*	0.0040(9)	0.0070(10)	0.0110(10)	0	−0.0012(8)	0
O2	4*c*	0.0046(9)	0.0078(9)	0.0057(9)	0	0.0001(8)	0
O3	4*c*	0.0049(10)	0.0085(9)	0.0052(9)	0	−0.0008(8)	0
O4	8*d*	0.0040(7)	0.0068(7)	0.0099(7)	0.0001(5)	−0.0007(5)	0.0003(5)
O5	8*d*	0.0047(7)	0.0086(7)	0.0051(6)	0.0001(5)	0.0000(5)	−0.0003(5)
O6	8*d*	0.0052(6)	0.0081(7)	0.0054(6)	0.0005(5)	0.0000(5)	−0.0003(5)
O7	4*c*	0.0051(9)	0.0064(9)	0.0052(9)	0	−0.0005(8)	0
O8	8*d*	0.0045(7)	0.0065(7)	0.0048(7)	0.0002(5)	−0.0002(5)	0.0000(5)
M=Ta							
Ta1	4*c*	0.00344(9)	0.00440(9)	0.00518(9)	0	−0.00045(6)	0
Mg1	8*d*	0.0046(4)	0.0035(5)	0.0040(4)	0.0001(3)	−0.0023(3)	0.0008(3)
Mg2	8*d*	0.0051(4)	0.0065(5)	0.0067(4)	0.0001(3)	−0.0013(4)	−0.0006(3)
Mg3	4*c*	0.0053(6)	0.0072(6)	0.0063(6)	0	0.0000(5)	0
O1	4*c*	0.0026(12)	0.0083(13)	0.0141(14)	0	−0.0036(11)	0
O2	4*c*	0.0039(12)	0.0074(13)	0.0054(12)	0	−0.0006(10)	0
O3	4*c*	0.0041(12)	0.0093(12)	0.0043(11)	0	0.0003(10)	0
O4	8*d*	0.0031(9)	0.0077(10)	0.0104(10)	−0.0005(7)	−0.0011(7)	0.0003(7)
O5	8*d*	0.0052(9)	0.0081(9)	0.0049(8)	0.0000(6)	0.0003(7)	0.0000(8)
O6	8*d*	0.0033(8)	0.0084(9)	0.0052(9)	0.0010(7)	0.0006(7)	−0.0004(7)
O7	4*c*	0.0041(12)	0.0051(13)	0.0062(12)	0	0.0004(10)	0
O8	8*d*	0.0039(9)	0.0051(9)	0.0043(8)	−0.0010(7)	−0.0012(7)	−0.0006(6)

Values of U_{12} and U_{23} at the 4*c* special positions are zero.

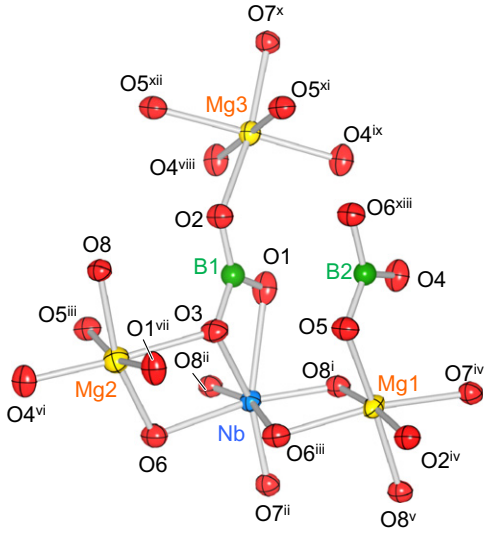

Fig. 1. Atomic arrangement around Mg, Nb, B and O atoms in the structure of $Mg_5NbO_3(BO_3)_3$. Displacement ellipsoids are drawn at the 99% probability level. Symmetry codes: (i) $x-1/2, -y+1/2, -z+1/2$; (ii) $x-1/2, y, -z+1/2$; (iii) $x, -y+1/2, z$; (iv) $-x+1/2, -y+1, z-1/2$; (v) $-x+1/2, y+1/2, z-1/2$; (vi) $x+1/2, -y+1/2, -z+1/2$; (vii) $x+1/2, y, -z+1/2$; (viii) $-x, y-1/2, -z+1$; (ix) $-x, -y+1, -z+1$; (x) $x-1/2, y, -z+3/2$; (xi) $-x+1/2, -y+1, z+1/2$; (xii) $-x+1/2, y-1/2, z+1/2$; and (xiii) $-x+1/2, y+1/2, z+1/2$.

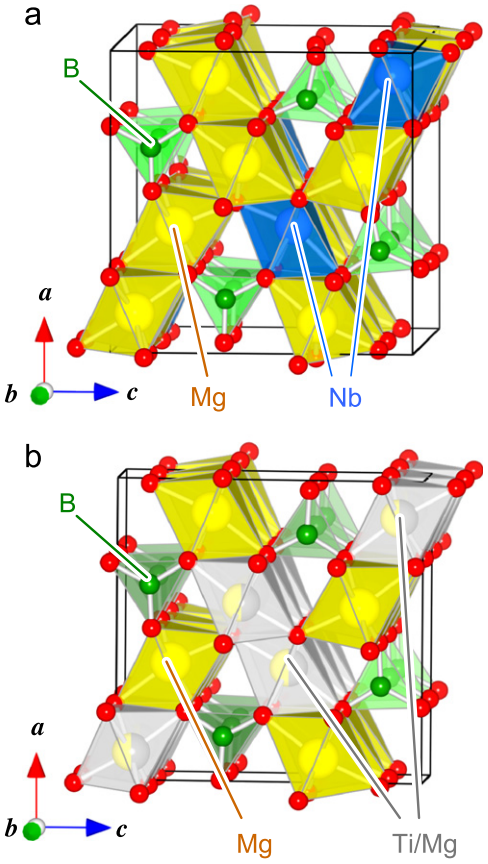

Fig. 2. Crystal structures of (a) $Mg_5NbO_3(BO_3)_3$ and (b) $Mg_3TiO_2(BO_3)_2$.

of our knowledge, $Mg_5NbO_3(BO_3)_3$ is the first photoluminescent solid state compound containing isolated NbO_7 polyhedra, while seven-coordinated Nb atoms have been known for some compounds as mentioned above.

In the structure of $Mg_4Nb_2O_9$ showing relatively small half widths of the excitation and emission peaks, isolated face-sharing dioctahedra of $^0[Nb_2O_9]^{8-}$ are surrounded by Mg atoms [39]. NbO_6 octahedra of $MgNb_2O_6$ share the edges and apexes and form $^2_\infty[Nb_2O_6]^{2-}$ layers, which are separated by Mg atom layers [40]. The widths of the excitation and emission peaks were broad compared to those of $Mg_4Nb_2O_9$. In $Mg_5NbO_3(BO_3)_3$ structure, an isolated NbO_7 polyhedron is surrounded by six Mg and three B

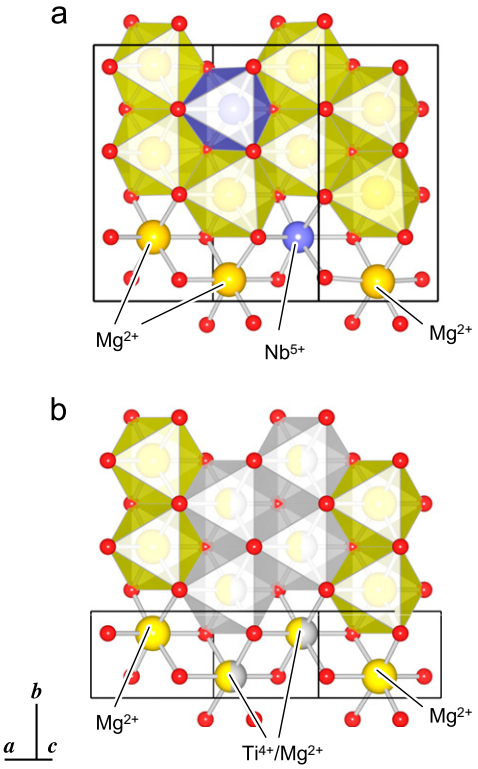

Fig. 3. Atomic arrangement in the layers composed of the M_4O_{18} units of (a) $Mg_5NbO_3(BO_3)_3$ and (b) $Mg_3TiO_2(BO_3)_2$.

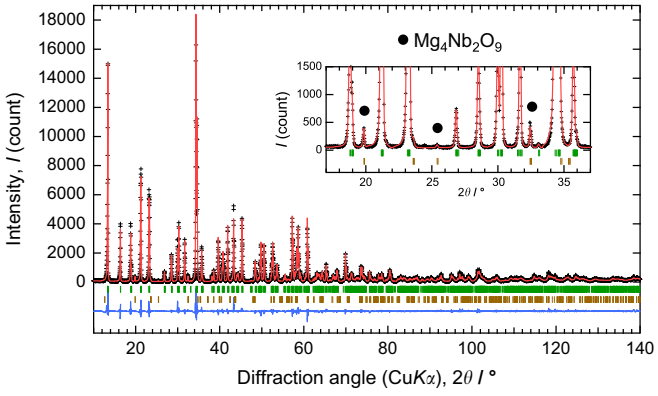

Fig. 4. Observed (crosses) and calculated (solid line) powder XRD patterns of $Mg_5NbO_3(BO_3)_3$. Less than 1 mass% of $Mg_4Nb_2O_9$ was contained as a second phase. Upper and lower vertical lines show all possible Bragg reflections of $Mg_5NbO_3(BO_3)_3$ and $Mg_4Nb_2O_9$, respectively. Difference between calculated and observed intensities is shown at the bottom of the figure.

atoms. However, four of the seven oxygen atoms of the polyhedron are bonded to B with high covalency. The coordination by O^{2-} oxide anions and O atoms of BO_3^{3-} groups might cause the broader peaks of excitation and emission. The red shift of the emission peak position observed from 385 to 470 nm might be related to the decrease of the average Nb–O distance (2.005 Å in $Mg_4Nb_2O_9$, 2.015 Å in $MgMn_2O_6$, and 2.100 Å in $Mg_5NbO_3(BO_3)_3$).

Broad emission at ~350 nm was observed from a mixture of $Mg_5TaO_3(BO_3)_3$, $Mg_4Ta_2O_9$ and MgO under ~230 nm excitation. The PL spectra were similar to those of $Mg_4Ta_2O_9$ at room temperature reported by Blasse and Bril [41]. Thus, the majority of the emission was considered to be from $Mg_4Ta_2O_9$ in the sample.

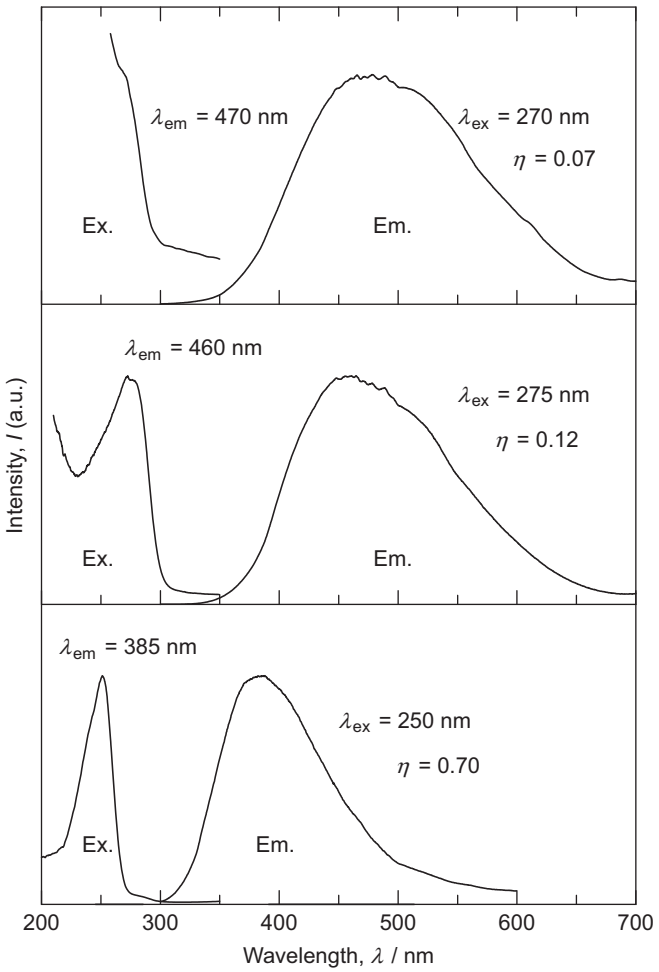

Fig. 5. PL excitation and emission spectra of (a) $Mg_5NbO_3(BO_3)_3$, (b) $MgNb_2O_6$ and (c) $Mg_4Nb_2O_9$ measured at room temperature.

4. Conclusion

In the MgO–$M^V_2O_5$–B_2O_3 (M^V=Nb, Ta) systems, single crystals of two new oxyborates, $Mg_5NbO_3(BO_3)_3$ and $Mg_5TaO_3(BO_3)_3$, were prepared at 1370 °C in air using B_2O_3 as a flux, and the polycrystalline sample of $Mg_5NbO_3(BO_3)_3$ was prepared at 1200 °C in air by solid state reaction. Both oxyborates have seven-coordinated Nb/Ta atoms and crystallize in the orthorhombic system with novel warwickite-type superstructures. $Mg_5NbO_3(BO_3)_3$ shows broad blue-to-green emission with a peak wavelength of 470 nm under 270-nm excitation.

Acknowledgment

This work was supported in part by the Global COE Program "Materials Integration, Tohoku University" and by a Grant-in-Aid for Scientific Research (B) (No. 21350113, 2009) from the Ministry of Education, Culture, Sports and Technology (MEXT), Japan.

Appendix A. Supplementary material

Supplementary data associated with this article can be found in the online version at doi:10.1016/j.jssc.2011.07.022.

References

[1] G. Heller, Top. Curr. Chem. 131 (1986) 39–98.
[2] J.D. Grice, P.C. Burns, F.C. Hawthorne, Can. Mineral. 37 (1999) 731–762.
[3] P. Becker, Adv. Mater. 10 (1998) 979–992.
[4] D.A. Keszler, Curr. Opin. Solid State Mater. Sci. 4 (1999) 155–162.
[5] S. Schmid, R.L. Withers, D. Corker, P. Baules, Acta Crystallogr., Sect. B: Struct. Sci. 56 (2000) 558–564.
[6] T. Ikeda, S. Fujiyoshi, H. Kato, A. Kudo, H. Onishi, J. Phys. Chem. B 110 (2006) 7883–7886.
[7] V.I. Voronkova, E.P. Kharitonova, V.K. Yanovskiĭ, S.Y. Stefanovich, A.V. Mosunov, N.I. Sorokina, Crystallogr. Rep. 45 (2000) 816–820.
[8] R.B. Guimarães, J.C. Fernandes, M.A. Continentino, H.A. Borges, C.S. Moura, J.B.M. da Cunha, C.A. dos Santos, Phys. Rev. B: Condens. Matter Mater. Phys. 56 (1997) 292–299.
[9] M.A. Continentino, A.M. Pedreira, R.B. Guimarães, M. Mir, J.C. Fernandes, R.S. Freitas, L. Ghivelder, Phys. Rev. B: Condens. Matter Mater. Phys. 64 (2001) 014406-1–014406-6.
[10] W.H.M.M. van de Spijker, W.L. Konijnendijk, Inorg. Nucl. Chem. Lett. 14 (1978) 389–392.
[11] G. Blasse, J. Inorg. Nucl. Chem. 31 (1969) 1519–1521.
[12] G. Blasse, Struct. Bonding 42 (1980) 1–41.
[13] A. Wachtel, J. Electrochem. Soc. 111 (1964) 534–538.
[14] G. Blasse, A. Bril, Z. Phys. Chem. N.F 57 (1968) 187–202.
[15] G. Blasse, A. Bril, J. Lumin. 3 (1970) 109–131.
[16] G. Blasse, J. Solid State Chem. 72 (1988) 72–79.
[17] G. Blasse, G.J. Dirksen, P. Zhiwu, G. Wehrum, R. Hoppe, Chem. Phys. Lett. 215 (1993) 363–366.
[18] G. Blasse, G.J. Dirksen, D.J.W. Ijdo, Mater. Res. Bull. 18 (1983) 721–726.
[19] G. Blasse, G.J. Dirksen, Phys. Stat., Sol. (a) Appl. Mater. Sci. 87 (1985) K181–K184.
[20] G. Blasse, G.J. Dirksen, Inorg. Chim. Acta 157 (1989) 141–142.
[21] G. Blasse, G.J. Dirksen, M.P. Crosnier, Y. Piffard, J. Alloys Compd. 189 (1992) 259–261.
[22] A.M. Srivastava, J.F. Ackerman, W.W. Beers, J. Solid State Chem. 134 (1997) 187–191.
[23] I.P. Roof, S. Park, T. Vogt, V. Rassolov, M.D. Smith, S. Omar, J. Nino, H.-C. zur Loye, Chem. Mater. 20 (2008) 3327–3335.
[24] M. Bharathy, V.A. Rassolov, S. Park, H.-C. zur Loye, Inorg. Chem. 47 (2008) 9941–9945.
[25] M. Bharathy, V.A. Rassolov, H.-C. zur Loye, Chem. Mater. 20 (2008) 2268–2273.
[26] PROCESS-AUTO; Rigraku/MSC & Rigaku Corporation: The Woodlands, TX, USA and Akishima, Tokyo, Japan, 2005.
[27] T. Higashi, NUMABS-Numerical Absorption Correction, Rigaku Corporation, Tokyo, 1999.
[28] L. Palatinus, G. Chapuis, J. Appl. Crystallogr. 40 (2007) 786–790.
[29] G.M. Sheldrick, Acta Crystallogr., Sect. A: Found. Crystallogr. 64 (2008) 112–122.
[30] L.J. Farrugia, J. Appl. Crystallogr. 32 (1999) 837–838.
[31] L.M. Gelato, E. Parthé, J. Appl. Crystallogr. 20 (1987) 139–143.
[32] F. Izumi, K. Momma, Solid State Phenom. 130 (2007) 15–20.
[33] K. Momma, F. Izumi, J. Appl. Crystallogr. 41 (2008) 653–658.
[34] I.D. Brown, D. Altermatt, Acta Crystallogr., Sect. B: Struct. Sci. 41 (1985) 244–247.
[35] N.E. Brese, M. O'Keeffe, Acta Crystallogr., Sect. B: Struct. Sci. 47 (1991) 192–197.
[36] R. Hofmann, R. Gruehn, Z. Anorg. Allg. Chem. 590 (1990) 81–92.
[37] I.E. Grey, W.G. Mumme, R.S. Roth, J. Solid State Chem. 178 (2005) 3308–3314.
[38] T. Kawano, H. Yamane, Acta Crystallogr., Sect. E: Struct. Rep. Online 67 (2011) i18–i19.
[39] N. Kumada, K. Taki, N. Kinomura, Mater. Res. Bull. 35 (2000) 1017–1021.
[40] S. Pagola, R.E. Carbonio, J.A. Alonso, M.T. Fernández-Díaz, J. Solid State Chem. 134 (1997) 76–84.
[41] G. Blasse, A. Bril, J. Solid State Chem. 3 (1971) 69–74.